EFFECT OF BOTTOM-SURFACE REFLECTIONS ON BACKSCATTER FROM POROSITY IN A COMPOSITE LAYER

T. Ohyoshi
Department of Mechanical Engineering
Akita University
Akita, 010, Japan

J. D. Achenbach
The Technological Institute
Northwestern University
Evanston, IL 60208

INTRODUCTION

Polar backscattering from a fiber-reinforced composite which contains regions of porosity, has been investigated in a number of papers [1]-[7]. Several scattering mechanisms appear to contribute to the backscattered signal. Roughly speaking the components of the backscattered signal can be attributed to effects of finite beam width, to the structuring of the material and to the existence of porosity.

It has been shown experimentally, [3]-[6], that polar backscatter from a multi-ply composite shows an amplitude dependence on the azimuthal angle which is characterized by a pattern of peaks and valleys. The peaks occur when the propagation vector of the incident pulse is normal to the direction of the fibers in one of the plies of the multi-ply layup. A theoretical model which accounts for this effect was proposed in Refs.[4] and [7]. Since the wavelengths at which the effect occurs is large as compared to the cross-sectional dimension of a fiber, the scattering action of single fibers was discounted in the discussion of Refs.[4] and [7]. It was, however, noted that a cross-sectional area of a fiber reinforced composite tends to show that the fibers are not uniformly spaced. There appears to be regions where the fibers are closely packed, while in other areas there is greater spacing. In Ref.[4] it was postulated that the deviations from relatively uniform fiber spacing act as scattering centers, which produce the steep variations in backscatter with azimuthal angle. Since it may be expected that the mechanical properties of the material in these irregular regions are close to those of the surrounding material, the Born approximation was used to investigate the polar backscattering from these inhomogeneities.

One effect, which has not yet been considered in the context of polar backscattering, concerns the influence of reflections from the bottom surface of a specimen. Fiber-reinforced composites display a great deal of attenuation of propagating disturbances due to the structuring of the material, due to porosity and due to the constitutive behavior of the fiber and matrix materials. Hence in some composites the ultrasonic wave motion may not have a significant amplitude when it reaches the bottom face of a composite specimen. The work reported in

Refs.[4] and [7], which ignores bottom-face reflections then applies directly. On the other hand, in other cases, particularly when the specimen is thin and/or the attenuation is not that large, the insonification of the bottom face will produce a reflection, which may contain useful information. Hence, in this paper the backscatter produced by the bottom surface of a specimen is discussed in some detail. Since, as follows from Refs.[4] and [7], the "peaks and valleys" effect due to inhomogeneities in the structuring is additive, it is not necessary to consider it in the present work. It can be added if this should be desirable. The emphasis in the present paper is, therefore, focussed on the backscatter from the upper and lower faces of the specimen, and on backscatter from porosity.

It is assumed in this study that the wavelength is sufficiently larger than the ply thickness. Hence, scattering by individual fibers and by the layered structure can be ignored. Hence, the composite is considered as a homogeneous but anisotropic layer.

The analysis presented in this paper requires the synthesis of several separate components. The composite has to be characterized as an anisotropic solid, the effective constants have to be computed, and the relations between phase velocities, propagation vectors, vectors defining the particle motion, as well as the propagation directions of the energy fluxes must be computed in terms of the effective elastic constants. Next the reflection and transmission coefficients at the water-solid interface must be obtained. Here the appearance of certain critical angles imposes severe limitations on the nature of the wave motion that can generated in the composite. The presence of both an upper and a lower solid-water interface generates multiple reflections, which must be considered. Finally the backscatter from the porosity must be analyzed. Here we first consider a single flat pore, which is characterized as a penny-shaped crack. Next the total effect of a distribution of pores is obtained by integration around the central ray of the incident beam.

The calculations associated with the analysis of the backscattered field, as described above, are lengthy. None of the details can be included in this brief presentation.

The geometry is shown in Fig. 1. A layer of the composite of thickness h is submerged in a water bath. The position of the transducer is defined by a polar angle θ_w.

SIGNAL STRENGTH FORMULAS

For a transducer system, Auld [8] has derived a steady-state reciprocal relation which can be applied to flaw detection and characterization. For backscattering (pulse-echo system) this relation gives the following expression for the change of received electrical signal due to the presence of an imperfection:

$$\delta\Gamma = \frac{i\omega}{4P} \int_S (\sigma_{k\ell} u_k^{in} - \sigma_{k\ell}^{in} u_k) n_\ell dA \ . \qquad (1)$$

Here S is an arbitrary surface which surrounds the imperfection, n_ℓ is the normal of the surface S ($\underset{\sim}{n}$ is defined positive inward), and P defines the power of the transducer. Also

$\sigma_{k\ell}^{in}, u_k^{in}$ correspond to the incident field

$\sigma_{k\ell}, u_k$ correspond to the perturbed field

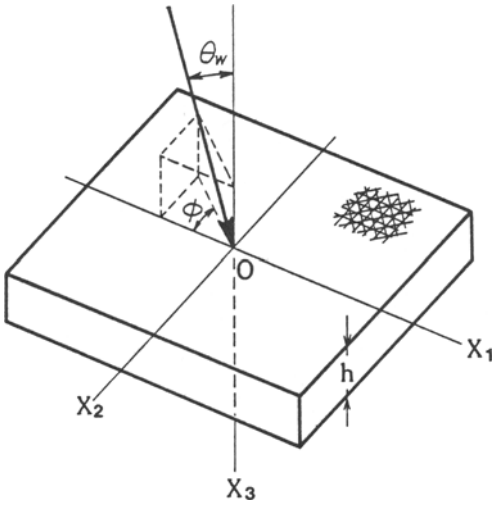

Fig. 1 Polar backscatter geometry

For backscattering by a crack, Eq.(1) reduces to

$$\delta\Gamma = \frac{i\omega}{4P} \int_{A+} \sigma^{in}_{k\ell} u_k \Delta u_k n_\ell dA \ , \tag{2}$$

where Δu_k is the crack-opening displacement, and the + sign defines the insonified crack face. From the top surface of the specimen we obtain

$$\delta\Gamma_t = \frac{i\omega}{4P} \int_{\Omega_t} (\sigma_{k3} u^{in}_k \Delta u_k - \sigma^{in}_{k3} u_k) d\Omega \ , \tag{3}$$

where Ω_t is the relevant area of interjection. Similarly for the bottom surface we have

$$\delta\Gamma_b = \frac{i\omega}{4P} \int_{\Omega_b} (\sigma_{33}\bar{u}_3 - \bar{\sigma}_{13} u_1 - \bar{\sigma}_{33} u_3) d\Omega \ , \tag{4}$$

Here $\bar{\sigma}_{k\ell}, \bar{u}_k$ corresponds to field transmitted into solid.

WAVE MOTION IN THE EFFECTIVE TRANSVERSELY ISOTROPIC MATERIAL

We assume that the mechanical behavior of the fiber reinforced composite may be represented by a transversely isotropic solid, whose axis of symmetry is in the x_3-direction. The origin of the coordinate system is located in the top (insonified) plane of the layer, as shown in Fig. 1. The material behaves in an isotropic manner in the x_1x_2-plane.

Let us consider a plane wave of the form

$$\underset{\sim}{u} = A \, \underset{\sim}{d} \exp (ik\underset{\sim}{p}\cdot\underset{\sim}{x}), \quad k = \omega/c \tag{5a,b}$$

An interesting feature of wave propagation in an anisotropic solid is that the direction of the energy flux vector, which defines the direction of energy flow, generally does not coincide with the direction of the phase propagation. The energy flux vector is defined by

$$< F_j > = - \frac{1}{T} \int_{t_o}^{t_o+T} \mathrm{Re}(\sigma_{ij}) \mathrm{Re}(v_i) dt \ , \qquad (6)$$

where $T = 2\pi/\omega$ is the period and $v_i = -i\omega u_i$ is the particle velocity. By the use of Eq.(5), $< F_j >$ can be expressed as

$$< F_j > = \frac{|A|^2}{2c} \omega^2 \ \mathrm{Re}(C_{mjk\ell} d_k p_\ell d_m^*) \ , \qquad (7)$$

where the asterisk indicates a complex conjugate, and $C_{mjk\ell}$ are the elastic constants of the anisotropic solid.

In the sequel we have sometimes used the following two-dimensional (plane strain) stress-strain relation

$$\begin{Bmatrix} \sigma_{11} \\ \sigma_{33} \\ \sigma_{31} \end{Bmatrix} = \begin{pmatrix} C_{11} & C_{13} & 0 \\ C_{13} & C_{33} & 0 \\ 0 & 0 & 2C_{55} \end{pmatrix} \begin{Bmatrix} \epsilon_{11} \\ \epsilon_{33} \\ \epsilon_{31} \end{Bmatrix} \qquad (8)$$

TRANSMISSION ACROSS THE WATER-SOLID INTERFACE

The reflection and transmission of a plane time-harmonic wave at an interface defined by $x_3 = 0$ of water and a transversely isotropic solid has been considered in Ref.[4]. The waves transmitted into the solid may be expressed as

$$\underset{\sim}{u} = T_\alpha \underset{\sim}{d}^\alpha \exp(ik_\alpha \underset{\sim}{p}^\alpha \cdot \underset{\sim}{x}), \quad \alpha = L, TV, TH \qquad (9)$$

Here T_α are the transmission coefficients. The transmission of wave motion into the solid has some interesting features at critical values of the angle of incidence θ_w (see Fig. 1). As θ_w increases beyond a first critical value, the propagation vector of the transmitted pseudo longitudinal wave becomes parallel to the water-solid interface, and the amplitude decays exponentially with depth into the solid. Similar effects happen at higher values of θ_w for the transmitted pseudo transverse waves. Hence at higher values of θ_w relatively little wave motion will penetrate to any depth into the composite.

Experimental measurements of the transmission of wave motion into unidirectionally reinforced composites of the kind considered here are often for the transmission of energy flux through the thickness of a plate. Corresponding expressions for coefficients of energy transmission can be derived by the use of Eqs.(7)-(9). We define

$$T_\alpha^E = \frac{\text{transmitted energy flux for } \alpha \text{ wave}}{\text{incident energy flux}} \ , \ \alpha = L, TV, TH \qquad (10)$$

The direction of energy flux in the solid is defined by the unit vector

$$\underset{\sim}{s}^\alpha = < \underset{\sim}{F}^\alpha > \ / |\underset{\sim}{F}^\alpha| \ , \quad \alpha = L, TV, TH \qquad (11)$$

Let us consider an area ΔA on the interface. The corresponding normal cross-sectional area of the incident wave (propagation vector $\underset{\sim}{p}^{in}$) in the water is $\Delta A p_3^{in}$, while the corresponding normal cross-sectional area in the solid is $\Delta A_\alpha = \Delta A \, s_3^\alpha$. We may then write Eq.(10) as

$$T_\alpha^E = |T_\alpha|^2 \frac{c_w}{c_\alpha} \frac{s_3^\alpha}{p_3^{in}} \mathrm{Re} \left(\frac{C_{mjk\ell}}{\lambda_w} d_k^\alpha \, p_\ell^\alpha (d_m^\alpha)^* \, s_j^\alpha \right) \qquad (12)$$

where T_α are the regular transmission coefficients defined in Eq.(9) and computed in Ref.[4].

MULTIPLE REFLECTIONS IN THE LAYER

Since the angle of incidence is taken to be beyond the critical angle, only pseudo-transverse waves, with propagation vector $\underline{p}^T$ and displacement vector $\underline{d}^T$, will penetrate to any depth in the layer. This simplifies the analysis of multiple reflections considerably, since only one kind of wave motion needs to be considered, and mode conversion can be neglected. It can then be shown that the relevant stress components in the solid can be expressed as

$$\hat{\sigma}_{13} = AC_{55}\, ik_w \tau_{13} E_R E_x \epsilon_x Z_- \tag{13}$$

$$\hat{\sigma}_{33} = AC_{55}\, ik_w \tau_{33} E_R E_x \epsilon_x Z_+ \tag{14}$$

where A is an amplitude function which can include the distribution across a possible beam width. The remainder of Eqs.(13)-(14) represent the plane wave part of the displacement. The constant C_{55} is a material constant, while

$$Z_\pm = \frac{1 \pm R_T^T H\, X^{-1}}{1 - (R_T^T)^2 H}\ , \tag{15}$$

where

$$H = \exp(2ik_T p_3^T h)\exp[-2(\tfrac{1}{2} N\sigma + \gamma)h/p_3] \tag{16}$$

$$X = \exp(2ik_T p_3^T x_3)\exp[-2(\tfrac{1}{2} N\sigma + \gamma)x_3/p_3] \tag{17}$$

Also

$$\tau_{13} = (p_1^T d_3^T + p_3^T d_1^T)(k_T/k_w) + i(d_1^T/p_3^T)(\tfrac{1}{2} N\sigma + \gamma)/k_w \tag{18}$$

$$\tau_{33} = (C_{13} p_1^T d_1^T + C_{33} p_3^T d_3^T)(k_T/k_w)/C_{55} + i(d_3^T/p_3^T)(\tfrac{1}{2} N\sigma + \gamma)(C_{33}/C_{55})/k_w \tag{19}$$

$$E_R = \exp(ik_w \underline{p}^{in} \cdot R) \tag{20}$$

$$E_x = \exp(ik_T \underline{p}^T \cdot x) \tag{21}$$

$$\epsilon_x = \exp[-(\tfrac{1}{2} N\sigma + \gamma)x_3/p_3^T] \tag{22}$$

The terms in Eqs.(16)-(17) include damping due both to scattering and material behavior. Generally there would be quantities σ_+ σ_-, which would be the scattering cross sections for forward scattering and backscatter from porosity. Here they are taken equal to σ; also, N is the number of pores per unit volume, and γ is the attenuation coefficient of the bulk composite.

BACKSCATTER FROM A CRACK

The signal strength of the backscattered field follows from Eq.(2). When the wavelength of the incident wave is much longer than the crack radius, the crack opening displacement for a crack located in a plane normal to the x_3-axis may be written as

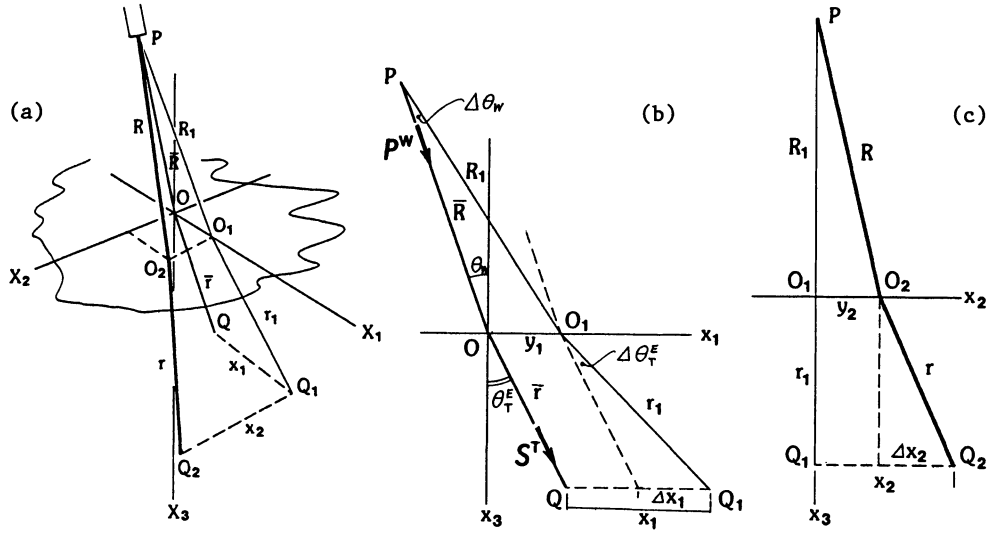

Fig. 2 Ray geometries for transmission across the water-solid interface.

$$\Delta u_j = \hat{\sigma}_{j3} f_j(x_1, x_2; \omega) \ , \tag{23}$$

where $\hat{\sigma}_{j3}$ is the (uniform) effective stress acting on the crack faces. Equation (2) then simplifies to

$$\delta\Gamma = -\frac{i\omega}{4P}(\sigma_{13}\hat{\sigma}_{13}V_1 + \sigma_{33}\hat{\sigma}_{33}V_3) \tag{24}$$

where V_j is the crack-opening volume per unit applied stress $\hat{\sigma}_{3j}$. For low frequency (long wavelength), the crack opening volume can be estimated.

The contributions from a number of cracks can be added to obtain the total signal, and this summation can subsequently be replaced by an integration, as discussed in Refs.[4] and [7]. These integrations are carried out in the immediate vicinity of the central ray of the propagating beam. It is, therefore, necessary to calculate ray lengths near the central ray of the beam.

Figure 2 shows the geometry in a Cartesian coordinate system. Ray POQ is the central ray of energy propagation. The lengths $\bar{R}$ and $\bar{r}$ are the ray lengths in the water and in the solid. It is necessary to express the length PO_2Q_2, that is R+r, when the point Q_2 is slightly displaced from the point Q by a length $(x_1^2 + x_2^2)^{1/2}$. The analysis is divided into two steps. The first step is to express the length $\overline{PO_1}(=R)$ and $\overline{O_1Q_1}(= r_1)$ in terms of $\bar{R}$ and $\bar{r}$, using the geometry shown in Fig. 2b. Next $\overline{PO_2}(=R)$ and $\overline{O_2Q_2}(= r)$ are expressed as functions of R_1 and r_1, using the geometry of Fig. 2c.

The total backscattered signal consists of three components: backscatter from the porosity. The result is

$$\delta\Gamma_t = -\frac{i\omega}{4P}\{-NT_T^E C_{55}^2 k_w^2 \int_o^h [\tau_{13}^2 I(x_3)\epsilon_x^2 Z_-^2 V_1 + \tau_{33}^2 I(x_3)\epsilon_x^2 Z_+^2 V_3]dx_3$$

$$+ T_T^E C_{55} ik_w [[r_{13} d_1^T I(x_3) Z_+ + r_{33} d_3^T I(x_3) Z_- - r_{33} d_3^T I(x_3) Z_+] \epsilon_x^2]_{x_3=h}$$

$$- \sqrt{T_T^E}\ C_{55} ik_w [\frac{\rho_w C_w^2}{C_{55}} d_3^T I(x_3) Z_- - p_{33}^w r_{33} I(x_3) Z_+]_{x_3=0}\} \qquad (25)$$

where all quantities have been defined earlier, except for $I(x_3)$ which is defined as

$$I(x_3) = \int_\Omega E_R^2 E_x^2 dx_1 dx_2 \qquad (26)$$

This integral can be further simplified by using the Fresnel integral.

BOTTOM-SURFACE EFFECT

The results have been normalized by the backscatter from the top surface, which may be calculated as

$$|\delta\Gamma_o| = \bar{R}\pi/k_w \qquad (27)$$

Numerical calculations were carried out for

$$C_{11} = 99.45\ GP_a,\ C_{13} = 3.39\ GP_a\ ,\ C_{33} = 10.79\ GP_a$$
$$C_{55} = 6.16\ GP_a,\ \rho_s = 1.57\ \ g/cm^3 \qquad (28)$$

The term $N\sigma/2$ was approximated as

$$N\sigma/2 \simeq (Na^2)(k_T a)^4/2\ , \qquad (29)$$

while γ was taken as

$$\gamma = 5 \times 10^{-4}\ mm^{-1} \qquad (30)$$

The geometrical parameters are

Slab thickness $h = 0$ to 5.0 (mm),

Sensor distance $R = 10$ (mm),

Flaw radius $a = 0.07$ (mm),

Incident angle $\theta_w = 20$ (deg.),

Frequency $f = 2$ (MHz)

Results for $|\delta\Gamma/\delta\Gamma_o|$ are shown in Figs. 3a,b and for low Na^2, the results show strong oscillations when $|\delta\Gamma/\delta\Gamma_o|$ is plotted versus h. As the volume density of the porosity increases, i.e., as Na^2 becomes larger, the oscillatory behavior disappears, because the reflection from the back surface disappears. Larger values of Na^2 correspond to more damping, and a signal is attenuated when it has traversed the distance h twice.

ACKNOWLEDGMENT

This work was carried out in the course of research sponsored by ONR.

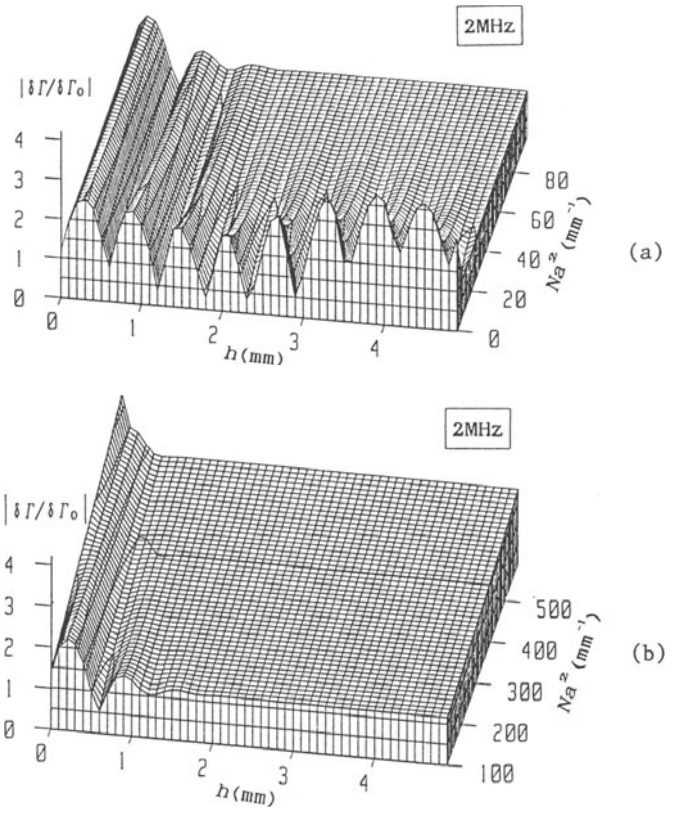

g. 3 Backscatter signal versus plate thickness and pore density at a frequency of 2 MHz.

REFERENCES

1. D. K. Hsu and S. M. Nair, in Review of Progress in Quantitative NDE, edited by D. O. Thompson and D. E. Chimenti (Plenum Press, New York, 1986), Vol. 6B, pp. 1185-1193.
2. R. A. Roberts, in Review of Progress in Quantitative NDE, edited by D. O. Thompson and D. E. Chimenti (Plenum Press, New York, 1986), Vol. 6B, pp. 1147-1156.
3. D. E. Yuhas, C. L. Vorres and R. A. Roberts, in Review of Progress in Quantitative NDE, 1986, edited by D. O. Thompson and D. E. Chimenti (Plenum Press, New York), Vol. 5B, p. 1275.
4. J. Qu and J. D. Achenbach, in Review of Progress in Quantitative NDE, edited by D. O. Thompson and D. E. Chimenti (Plenum Press, New York), Vol. 6B, pp. 1137-1146.
5. Y. Bar-Cohen and R. L. Crane, Material Evaluation, 40, 970-975 (1982).
6. E. D. Blodgett, L. J. Thomas III and J. G. Miller, in Review of Progress in Quantitative NDE, edited by D. O. Thompson and D. E. Chimenti (Plenum Press, New York, 1986), Vol. 5B, p. 1267.
7. J. Qu and J. D. Achenbach, in Review of Progress in Quantitative NDE, edited by D. O. Thompson and D. E. Chimenti (Plenum Press, New York), Vol. 7.
8. B. A. Auld, WAVE MOTION 1, 1979, pp. 3-5.